Universal tight-binding calculation for the electronic structure of the quaternary alloy $In_{1-x}Ga_xAs_{1-y}P_y$

Kyurhee Shim

Department of Chemistry, Princeton University, Princeton, New Jersey 08544
and Department of Physics, Kyonggi University, Suwon 440-760, Korea

Herschel Rabitz

Department of Chemistry, Princeton University, Princeton, New Jersey 08544

The energy band gaps and the density of states (DOS) of the quaternary alloy semiconductor $In_{1-x}Ga_xAs_{1-y}P_y$ lattice matched on InP and GaAs are calculated and analyzed by using the universal tight-binding (UTB) method based on a modified pseudocell (MPC). Good agreement was obtained between the calculated values and the experimental data for the lattice-matched alloy to InP, and a new band gap trend was observed for the lattice-matched alloy to GaAs. In addition, the entire composition variations of the Γ, L, and X band gaps for the $In_{1-x}Ga_xAs_{1-y}P_y$ alloy are obtained. The calculations suggest that the alloy $In_{1-x}Ga_xAs_{1-y}P_y$ in the low composition range of (x,y) and lattice matched to InP can be used for efficient light emitting devices, but not for lattice matching to GaAs. The origin of band bowing is interpreted as the atomic orbital interactions through the bond alternation. The anion mixing affects on the shift of the DOS peak position and the cation mixing plays a dominant role on the change of the DOS peak intensity in the conduction band. The theoretical model is generic and applicable to various quaternary alloy systems. [S0163-1829(98)05319-3]

I. INTRODUCTION

The III-V semiconducting alloys have received considerable attention for various semiconductor-device applications because their energy band structure and lattice parameters can be changed and fabricated independently. The electronic structure of semiconductor alloys plays a crucial role in determining their optoelectronic properties for devices such as lasers, light emitting diodes (LED), optical amplifiers, modulators, and detectors.[1-4] Recently developed techniques for growing crystalline random alloys, such as molecular beam epitaxy (MBE), liquid phase epitaxy (LPE), and metalorganic chemical vapor deposition (MOCVD), have stimulated theoretical and experimental research as well as device fabrication.[5-7]

In spite of an abundance of experimental work on the alloys, there has been little theoretical effort because of the computational difficulties and complexities that arise in dealing with the disorder in the alloys. The simplest approximation for the electronic structure of alloys is the virtual crystal approximation (VCA) in which the alloy potential is replaced by the concentration weighted average of the constituent potentials while neglecting compositional disorder effects. The coherent potential approximation (CPA) (Refs. 8 and 9) takes considerably better account of compositional disorder for the alloy by including the disorder effects in a single-site approximation in which the remainder of the crystal is still treated as a mean environment.[10] The CPA has provided good quantitative results for the electronic structures of alloys, but a comprehensive consideration of the range of disordered correlation and local atomic relaxation remains limited because of the computational complexity. Other approaches based on second-order perturbation theory

(SPT) (Ref. 11) and the semiempirical tight binding (SETB) methods[12] have been proposed, in which the disorder effects are incorporated semiempirically. These methods have yielded good results for the Γ energy gap compared to the experimental data. However, these methods have limitations as they require either experimental or theoretical data for the alloy system in order to fit the band bowing parameters. To the best of our knowledge, there does not exist any unified theory to predict the electronic structure of semiconductor alloys without suffering from computational complexity and/or employing experimental data. The universal tight binding method aims at presenting an efficient and accurate means to calculate the electronic structure of the alloy without those restrictions. The availability of reliable theoretical techniques for treating alloys is essential to improve device designs.

Previously, we have developed a universal tight binding method as a simple efficient method to predict the electronic structure of ternary alloy semiconductors[13] in which compositional disorder and lattice relaxation effects were incorporated by interpolating between the TB parameters of constituent semiconductors without recourse to experimental information. The calculated results of the main band gaps of ternary alloys were found to be in close agreement with experimentally determined energy values.

In this paper, we adopt similar methodology to investigate quaternary alloy systems $A_{1-x}B_xC_{1-y}D_y$ and propose the universal tight binding (UTB) method based on a modified pseudocell (MPC) to calculate the energy band structure and the density of states (DOS). The UTB method based on MPC treats the alloy in a simple fashion by replacing the alloy system with an effective-perfect bulk system, thereby allowing for a simplification to reduce the computational effort

without employing any empirical data. In order to demonstrate that UTB based on MPC can be readily applied to the quaternary alloy system, the case of $In_{1-x}Ga_xAs_{1-y}P_y$ alloys is analyzed.

The $In_{1-x}Ga_xAs_{1-y}P_y$ quaternary alloy, which can be lattice-matched to two of its constituent binaries—GaAs and InP—is one of the major materials for the fabrication of optoelectronic devices such as edge or surface emitting long wavelength semiconductor lasers.[1,6] The band gap of a quaternary alloy can change widely while maintaining the lattice match completely to a binary crystal used as a substrate. This paper presents the UTB values for the direct $[E(\Gamma)]$, the indirect $[E(L)$ and $E(X)]$, and the $E1$ energy gaps over the entire range of alloy composition for the $In_{1-x}Ga_xAs_{1-y}P_y$ alloy. Also, the band-gap trends of the alloy lattice-matched to InP and GaAs with certain x-y composition relationships between x and y are obtained and examined due to their potential value as efficient light emitting devices (ELED). In addition, the variation of the DOS has been analyzed over a range of x for fixed anion composition y and over a range of y for fixed cation x. These results enable us to distinguish the dominant role of anion and cation mixing in the quaternary alloy.

II. THEORY

Alloy semiconductors consist of more than two elements with a range of concentration ratios, in which the additional effect of disorder is taken into account as a compositional fluctuation. To reduce the computational efforts and simplify the complexity of the many-body problem, we propose using the MPC. The notion of a pseudocell was suggested by Chang[14] to describe the vibrational properties of ternary alloys, in which effective force constants represented the interaction between ions. The MPC in the quaternary alloy $A_{1-x}B_xC_{1-y}D_y$ is defined as consisting of four counterfeit ions of $(1-x)A$, xB, $(1-y)C$, and yD that interact with each other in the same manner as in the real alloy system as a function of the composition mixing probability ratio. There are four possible binary units AC, AD, BC, and BD with the mixing probability $(1-x)(1-y)$, $(1-x)y$, $x(1-y)$, and xy, respectively, and each binary unit is considered to be disordered by the other two ions, so that eight disordered units are taken into consideration such as AC:B, AC:D, AD:B, AD:C, BC:A, BC:D, BD:A, and BD:C. The quaternary alloy semiconductor is assumed to be formed by the repetition of the MPC containing two atoms in the cell. The MPC is a virtual cell attempting to retain the physical effects of reduced point-group symmetry and lattice distortion and to describe the alloy in a convenient manner.

Considering MPC, an arbitrary physical operator $(\hat{O}_{x,y}^{alloy})$ of the quaternary alloy $A_{1-x}B_xC_{1-y}D_y$ can be taken as follows:

$$\hat{O}_{x,y}^{alloy} = (1-x)(1-y)\hat{O}_{AC} + (1-x)y\hat{O}_{AD} + x(1-y)\hat{O}_{BC}$$
$$+ xy\hat{O}_{BD}, \qquad (1)$$

where

$$\hat{O}_{AC} = \hat{O}_{AC}^0 + \Delta\hat{O}_{AC}, \qquad (2)$$

$$\hat{O}_{AD} = \hat{O}_{AD}^0 + \Delta\hat{O}_{AD},$$

$$\hat{O}_{BC} = \hat{O}_{BC}^0 + \Delta\hat{O}_{BC},$$

$$\hat{O}_{BD} = \hat{O}_{BD}^0 + \Delta\hat{O}_{BD}.$$

$\hat{O}_{AC}^0$ is the nondisordered value for the AC compounds and $\Delta\hat{O}_{AC}$ is the disordered-AC values induced by B and D ions, which can be written as $\Delta\hat{O}_{AC} = \Delta\hat{O}_{AC:B} + \Delta\hat{O}_{AC:D}$, etc.

The crystalline TB Hamiltonian with zinc-blende structure has the Slater-Koster form and a Hamiltonian matrix element is

$$H_{mn} = \frac{1}{N}\sum_{R_i,R_j} e^{i\mathbf{k}\cdot(\mathbf{R}_i-\mathbf{R}_j)}\langle\psi_n(\mathbf{r}-\mathbf{R}_i)|\hat{H}|\psi_m(\mathbf{r}-\mathbf{R}_j)\rangle. \tag{3}$$

Here, $\psi_m(\mathbf{r}-\mathbf{R}_j)$ is the atomic orbital centered at the jth atom site $\mathbf{R}_j$ with the matrix element evaluated over $\mathbf{r}$ and the label m corresponds to s, p_x, p_y, and p_z describing the atomic orbitals. The basic operation in the TB framework is to find the matrix elements of the Hamiltonian between the various basis states, which are treated as TB parameters; $E_{mn}(\mathbf{R}_i-\mathbf{R}_j) = \langle\psi_n(\mathbf{r}-\mathbf{R}_i)|\hat{H}|\psi_m(\mathbf{r}-\mathbf{R}_j)\rangle$.

In the UTB method based on MPC, the Hamiltonian matrix elements for an alloy are determined by interpolating between the parent crystal TB parameters according to the alloy composition. This procedure is based on the assumption that the band structure of an alloy may be presented by the replacement of the real alloy with crystal forms that have the translation symmetry and the point-group symmetry of the parent crystals. Considering this assumption, the quaternary alloy Hamiltonian $\hat{H}_{A_{1-x}B_xC_{1-y}D_y}$ takes the form

$$\hat{H}_{A_{1-x}B_xC_{1-y}D_y} = (1-x)(1-y)\hat{H}_{AC} + (1-x)y\hat{H}_{AD}$$
$$+ x(1-y)\hat{H}_{BC} + xy\hat{H}_{BD}, \qquad (4)$$

where the effective Hamiltonian of the AC binary compound $(\hat{H}_{AC})$ can be written as the nondisordered Hamiltonian $(\hat{H}_{AC}^0)$ and the disordered Hamiltonian $(\Delta\hat{H}_{AC})$, such that $\hat{H}_{AC} = \hat{H}_{AC}^0 + \Delta\hat{H}_{AC}$, and similarly for the other binary compounds. Here, $\Delta\hat{H}_{AC}$ is the total disordered Hamiltonian induced by B ions $(\Delta\hat{H}_{AC:B})$ and D ions $(\Delta\hat{H}_{AC:D})$ with the composition x and y, respectively, etc., such that

$$\Delta\hat{H}_{AC} = x\Delta\hat{H}_{AC:B} + y\Delta\hat{H}_{AC:D},$$

$$\Delta\hat{H}_{AD} = x\Delta\hat{H}_{AD:B} + (1-y)\Delta\hat{H}_{AD:C},$$

$$\Delta\hat{H}_{BC} = (1-x)\Delta\hat{H}_{BC:A} + y\Delta\hat{H}_{BC:D},$$

$$\Delta\hat{H}_{BD} = (1-x)\Delta\hat{H}_{BD:A} + (1-y)\Delta\hat{H}_{BD:C}. \qquad (5)$$

Considering these effective Hamiltonians, the UTB Hamiltonian can be expressed as

$$\hat{H}_{A_{1-x}B_xC_{1-y}D_y} = (1-x)(1-y)\hat{H}^0_{AC} + (1-x)y\hat{H}^0_{AD}$$
$$+ x(1-y)\hat{H}^0_{BC} + xy\hat{H}^0_{BD}$$
$$+ (1-x)(1-y)yV_{ACD} + xy(1-y)V_{BCD}$$
$$+ x(1-x)(1-y)V_{ABC} + xy(1-x)V_{BAD}, \quad (6)$$

where V_{ACD} is the disordered energy in the $AC{:}D$ and $AD{:}C$ units, which can be approximated as the bond alternation energy between AC and AD binaries ($V_{ACD} = \Delta\hat{H}_{AC:D} + \Delta\hat{H}_{AD:C} \equiv \hat{H}^0_{AC} - \hat{H}^0_{AD}$), etc. The last four terms in Eq. (6) become the total disordered energy induced by ACD, BCD, ABC, and BAD units in the $A_{1-x}B_xC_{1-y}D_y$ alloy system and govern the extent of energy band-gap bowing. Therefore, the extent of the band-gap bowing depends on the differences of the bond energy between the constituent materials and corresponding compound compositions as in Eq. (6).

With this UTB Hamiltonian, the diagonalization of the secular matrix $\hat{H}$ provides the eigenvalues E_{nk} in the Bril-louin zone (BZ) for the quaternary alloys. From the calculated energy eigenvalues, the principal energy band gaps $[E(\Gamma), E(L), \text{ and } E(X)]$ due to the local conduction-band minima (valleys) are obtained by the difference between the minimum of the conduction bands ($E^c_{\min}$) at the Γ, L, and X symmetry points and the maximum of the valence bands ($E^v_{\max}$) at the Γ points: $E(\Gamma) = E^c_{\min}(\Gamma) - E^v_{\max}(\Gamma)$, $E(L) = E^c_{\min}(L) - E^v_{\max}(\Gamma)$, and $E(X) = E^c_{\min}(X) - E^v_{\max}(\Gamma)$. The $E1$ level is assumed to be induced by the transition from the minimum of the L conduction band to the maximum of the L valence band: $E1 = E^c_{\min}(L) - E^v_{\max}(L)$.

Each of the Hamiltonian matrix elements, which are called the universal tight-binding parameters (UTBP), can be expressed as an interpolation between the binary TB parameters according to compositional mixing probability. Harrison's scheme[15] is adopted in the UTBP, for the interatomic parameters with scaling as the inverse square of the bond length (d^{-2}), and the Slater and Koster TB parametrization[16] is retained with interactions up to second nearest neighbor. For $A_{1-x}B_xC_{1-y}D_y$ quaternary alloys, the compositional UTBP can be written as follows:

$$E_{mn}(x,y) = (1-x)(1-y)E^0_{AC,mn} + (1-x)yE^0_{AD,mn} + x(1-y)E^0_{BC,mn} + xyE^0_{BD,mn}$$
$$+ (1-x)y(1-y)\Delta E_{mn}(ACD) + xy(1-y)\Delta E_{mn}(BCD) + (1-y)x(1-x)$$
$$\times \Delta E_{mn}(ABC) + yx(1-x)\Delta E_{mn}(BAD) \quad (7)$$

for the intra-atomic and second-nearest-atomic matrix elements, and

$$\bar{d}^2(x,y)E_{mn}(x,y) = (1-x)(1-y)(d^0_{AC})^2E^0_{AC,mn} + (1-x)y(d^0_{AD})^2E^0_{AD,mn} + x(1-y)(d^0_{BC})^2E^0_{BC,mn} + xy(d^0_{BD})^2E^0_{BD,mn}$$
$$+ x(1-x)y(1-y)(\Delta d^0(ACD))^2\Delta E_{mn}(ACD) + xy(1-y)(\Delta d^0(BCD))^2\Delta E_{mn}(BCD)$$
$$+ x(1-x)(1-y)(\Delta d^0(ABC))^2\Delta E_{mn}(ABC) + x(1-x)y(\Delta d^0(BAD))^2\Delta E_{mn}(BAD) \quad (8)$$

for the interatomic matrix elements, where $\Delta d^0(ACD) = d^0_{AC} - d^0_{AD}$ and $\Delta E_{mn}(ACD) = E^0_{AC,mn} - E^0_{AD,mn}$, respectively, are the differences of bond lengths and TB matrix elements between the AC and AD binaries in the ACD disordered unit, etc. The composition average bond length $\bar{d}$ is used from Ref. 17.

The concentration variation of the density of states (DOS) $\rho(\varepsilon)$ is very important in alloy theory. The DOS is defined as

$$\bar{\rho}(\varepsilon) = \frac{1}{N}\sum \delta[\varepsilon - \varepsilon_n(k)], \quad (9)$$

where N is the total number of lattice sites in the crystal, and $\varepsilon_n(k)$ is the band energy of the $\hat{H}_{\text{alloy}}$ from the UTB method. For a given set of concentrations x and y, $\hat{H}_{\text{alloy}}$ is computed, and then the band energies of $\hat{H}_{\text{alloy}}$, $\varepsilon_n(k)$, are calculated on 457 grid points in the BZ.

III. NUMERICAL CALCULATIONS

We have carried out energy band calculations for the $In_{1-x}Ga_xAs_{1-y}P_y$ quaternary alloy in the entire range of x and y (Fig. 1) and for the lattice matched to InP and GaAs (Figs. 2 and 3), where the lattice-matched relations between x and y for InP and GaAs are used as obtained in Ref. 17. The TB parameters for the four constituent binary systems (InP, InAs, GaAs, and GaP) were mainly taken from the work of Talwar and Ting[18] and slight adjustments were made to account for more recent data on the experimental band structures. The main emphasis was placed on accurately reproducing the bands in the vicinity of the principal gap. The TB parameters and the bond lengths used in this work are listed in Table I.

The variation of the principal energy band gaps $[E(\Gamma), E(L), \text{ and } E(X)]$ for the $In_{1-x}Ga_xAs_{1-y}P_y$ on the entire range are quantitatively presented in Table II and shown in Figs. 1(a)–1(c). Three energy gaps are drawn within the same energy range in Fig. 1(d) and the composition relation of the crossover between the band gaps is projected onto the xy plane in Fig. 1(e). As can be seen in Fig. 1(d), the $E(X)$ change relatively slowly so that the $E(\Gamma)$ and $E(X)$ cross at the composition range of $y \sim \geqslant -0.83x + 1.41$ and become an indirect gap induced by $E(X)$. This implies that the $In_{1-x}Ga_xAs_{1-y}P_y$ quaternary alloy can be used as an effi-
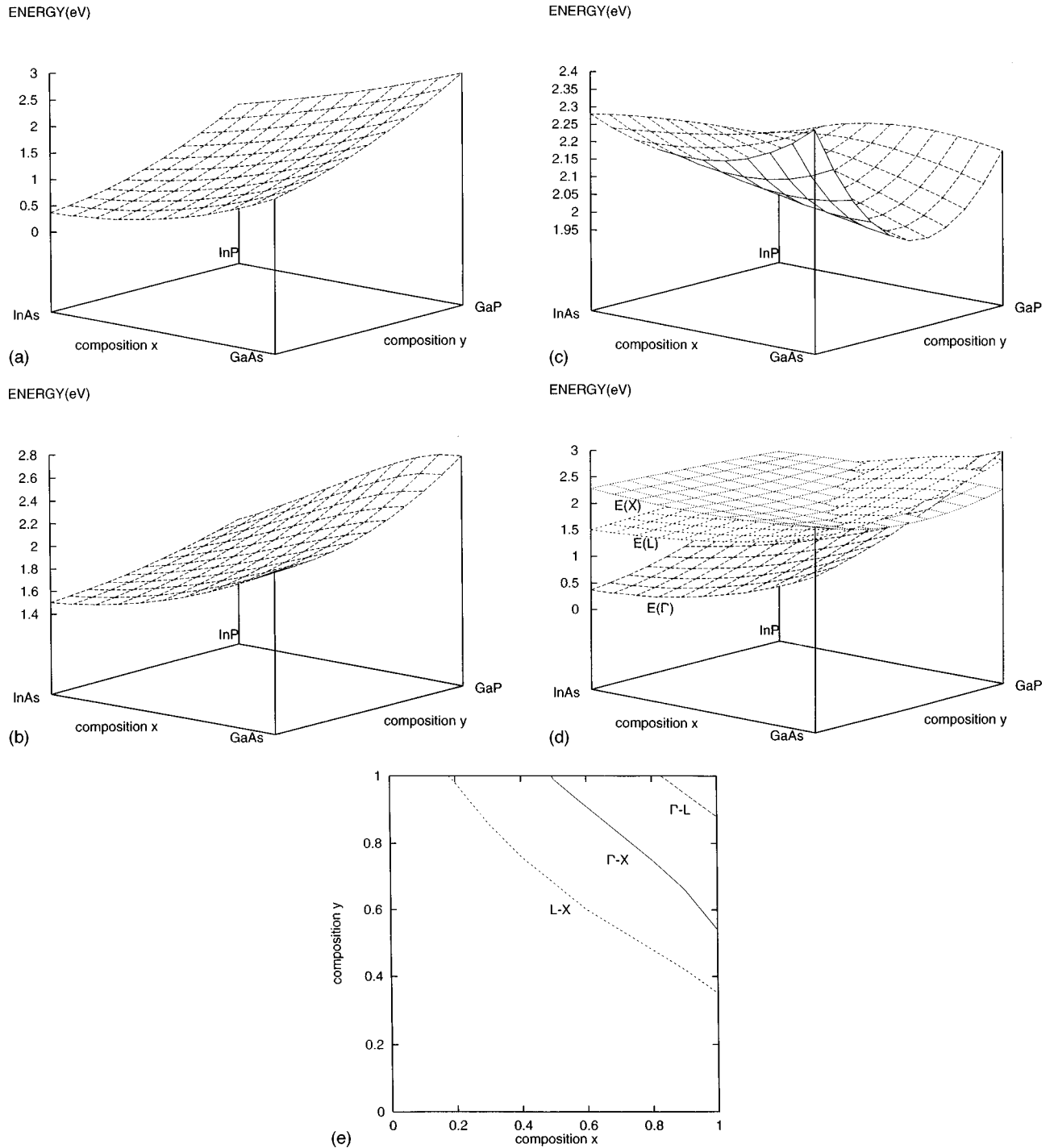
FIG. 1. (a) $E(\Gamma)$ energy gap variation over the entire range of alloy composition (x,y) for $\text{In}_{1-x}\text{Ga}_x\text{As}_{1-y}\text{P}_y$. (b) $E(L)$ energy gap variation over the entire range of alloy composition (x,y) for $\text{In}_{1-x}\text{Ga}_x\text{As}_{1-y}\text{P}_y$. (c) $E(X)$ energy gap variation over the entire range of alloy composition (x,y) for $\text{In}_{1-x}\text{Ga}_x\text{As}_{1-y}\text{P}_y$. (d) Three energy gap variations [$E(\Gamma)$, $E(L)$, and $E(X)$] over the entire range of alloy composition (x,y) for $\text{In}_{1-x}\text{Ga}_x\text{As}_{1-y}\text{P}_y$. (e) The projected crossover lines in the xy plane between the band gaps ($\Gamma-X$, $L-X$, and $\Gamma-L$) for $\text{In}_{1-x}\text{Ga}_x\text{As}_{1-y}\text{P}_y$.

cient light emitting device (ELED) at the low composition range (x,y) because it has the direct optical gap induced by $E(\Gamma)$ with a considerable distance from the $E(L)$ and $E(X)$ gap, in which the electron in the lowest conduction band recombines directly with a hole at the top of the valence band at the zone center(Γ) with the emission of a photon.

The $\text{In}_{1-x}\text{Ga}_x\text{As}_{1-y}\text{P}_y$ alloy can be lattice-matched to two of its constituent binaries InP and GaAs. No longer are x and

y independent of one another because the lattice constant of the alloy is adjusted to that of InP ($d^0_{\text{InP}}=2.541$ Å) or GaAs ($d^0_{\text{GaAs}}=2.448$ Å).[17] Consequently, the band gap can be obtained along the definite relationships between x and y composition. The relationships between x and y for the lattice matched to InP and GaAs were found to be linearly dependent on alloy composition x and y: $x=0.47(1-y)$ ($0\leqslant x \leqslant 0.47$, $0\leqslant y\leqslant 1.0$) for the alloy $\text{In}_{1-x}\text{Ga}_x\text{As}_{1-y}\text{P}_y$ lattice
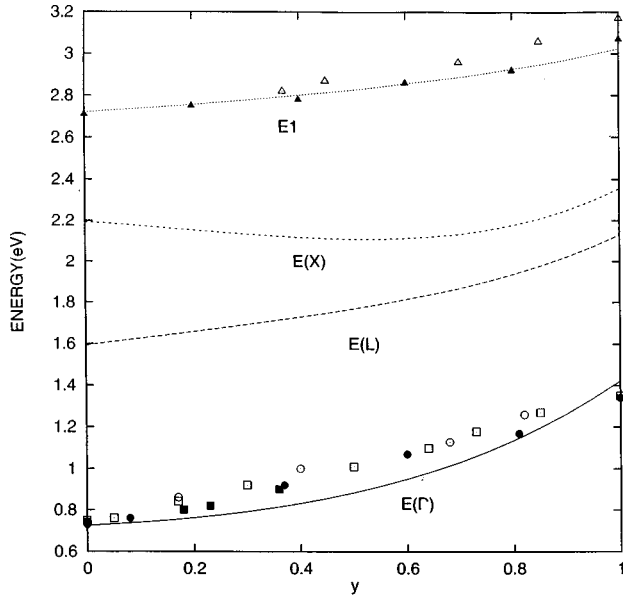
KYURHEE SHIM AND HERSCHEL RABITZ

FIG. 2. Γ, L, X, and $E1$ energy gap variations as a function of alloy concentration y with x chosen to be lattice-matched to InP for $In_{1-x}Ga_xAs_{1-y}P_y$. The calculated values are compared to experimental data: $\odot$ (Ref. 19), $\bullet$ (Ref. 20), $\boxdot$ (Ref. 21), $\blacksquare$ (Ref. 22), $\triangle$ (Ref. 23), and $\blacktriangle$ (Ref. 24).

matched to InP (Ref. 21) and $x = 1 - 0.45y$ ($0.55 \leq x \leq 1$, $0 \leq y \leq 1.0$) for the alloy $In_{1-x}Ga_xAs_{1-y}P_y$ lattice matched to GaAs.[17] Figures 2 and 3 present the variation of the principal
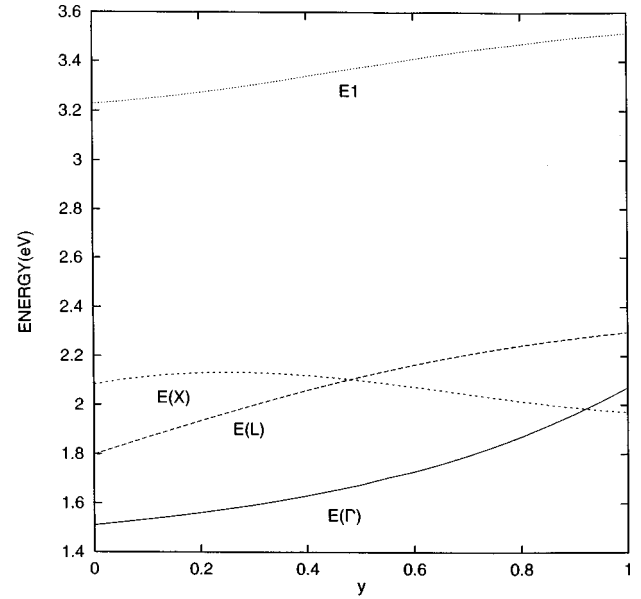
FIG. 3. Γ, L, X, and $E1$ energy gap variations as a function of alloy concentration y with x chosen to be lattice-matched to GaAs for $In_{1-x}Ga_xAs_{1-y}P_y$.

gaps and $E1$ level for the $In_{1-x}Ga_xAs_{1-y}P_y$ quatenary alloy lattice matched to InP and GaAs. The band-gap bowing behavior of the system is governed by the total disordered energy induced by the differences of bond energies between the constituent binaries and the relationship(combination) be-

TABLE I. TB parameters and bond lenghts of four binary compounds of the quaternary alloy $In_{1-x}Ga_xAs_{1-y}P_y$.

TB parameters and bondlength	InAs	InP	GaAs	GaP
$P_1 = E_{ss}(000)0$	-7.1793	-6.2941	-6.7236	-6.2848
$P_2 = E_{ss}(000)1$	-4.4868	-3.4287	-3.9783	-2.7892
$P_3 = E_{xx}(000)0$	1.6600	1.8429	0.6410	1.0943
$P_4 = E_{xx}(000)1$	2.3356	2.6089	2.8741	2.3820
$P_5 = 4E_{ss}(0.5, 0.5, 0.5)$	-6.4000	-6.2200	-6.9000	-7.7500
$P_6 = 4E_{sx}(0.5, 0.5, 0.5)01$	5.4000	4.7000	5.3000	5.2600
$P_7 = 4E_{sx}(0.5, 0.5, 0.5)10$	4.0000	4.3800	4.2500	4.9500
$P_8 = 4E_{xx}(0.5, 0.5, 0.5)$	2.0000	2.2800	2.0000	2.4400
$P_9 = 4E_{xy}(0.5, 0.5, 0.5)$	5.4600	5.3000	5.5000	5.5600
$P_{10} = 4E_{xx}(0,1,1)0$	-0.8241	-0.7202	-0.3391	-1.1376
$P_{11} = 4E_{xx}(0,1,1)1$	-1.2025	-1.3382	-1.7563	1.1861
$P_{12} + 4E_{xy}(1,1,0)0$	0.5500	0.5200	0.6000	0.7600
$P_{13} = 4E_{xy}(1,1,0)1$	0.8800	0.9100	0.9600	1.3300
$P_{14} = 4E_{xx}(1,1,0)0$	0.2274	0.3842	0.4445	0.8545
$P_{15} = 4E_{xx}(1,1,0)1$	0.9831	0.7391	1.1208	1.1892
$P_{16} = 4E_{sx}(1,1,0)0$	0.0560	0.0870	0.0452	0.0240
$P_{17} = 4E_{sx}(1,1,0)1$	0.0860	0.1020	0.0964	0.0832
$P_{18} = 4E_{ss}(1,1,0)0$	-0.0924	-0.0816	-0.0474	-0.1673
$P_{19} = 4E_{ss}(1,1,0)1$	-0.1256	-0.0342	-0.0653	-0.1814
$P_{20} = 4E_{sx}(0,1,1)0$	0.8400	0.9000	0.7800	1.1800
$P_{21} = 4E_{sx}(0,1,1)1$	-0.0800	-0.0060	-0.0800	-0.0800
$P_{22} = 4E_{xy}(0,1,1)0$	0.0	0.0	0.0	0.0
$P_{23} = 4E_{xy}(0,1,1)1$	0.0	0.0	0.0	0.0
d^0	2.623	2.541	2.448	2.358

TABLE II. Principal energy gap values over the entire range of (x,y) for $In_{1-x}Ga_xAs_{1-y}P_y$.

(x,y)	$E(\Gamma)$ (eV)	$E(L)$ (eV)	$E(X)$ (eV)	(x,y)	$E(\Gamma)$ (eV)	$E(L)$ (eV)	$E(X)$ (eV)
0.0,0.0	0.370	1.502	2.280	0.6,0.0	0.858	1.627	2.171
0.0,0.2	0.423	1.552	2.229	0.6,0.2	1.034	1.75	2.134
0.0,0.4	0.55	1.637	2.207	0.6,0.4	1.249	1.895	2.093
0.0,0.6	0.755	1.758	2.218	0.6,0.6	1.506	2.054	2.051
0.0,0.8	1.044	1.921	2.265	0.6,0.8	1.804	2.209	2.01
0.0,1.0	1.422	2.13	2.356	0.6,1.0	2.148	2.331	1.97
0.2,0.0	0.469	1.528	2.249	0.8,0.0	1.15	1.703	2.128
0.2,0.2	0.568	1.596	2.185	0.8,0.2	1.357	1.862	2.127
0.2,0.4	0.729	1.692	2.139	0.8,0.4	1.593	2.042	2.116
0.2,0.6	0.955	1.817	2.113	0.8,0.6	1.859	2.229	2.093
0.2,0.8	1.247	1.969	2.108	0.8,0.8	2.157	2.398	2.062
0.2,1.0	1.612	2.144	2.128	0.8,1.0	2.489	2.498	2.023
0.4,0.0	0.631	1.569	2.212	1.0,0.0	1.51	1.798	2.083
0.4,0.2	0.771	1.661	2.153	1.0,0.2	1.742	1.998	2.136
0.4,0.4	0.962	1.778	2.101	1.0,0.4	1.994	2.218	2.168
0.4,0.6	1.205	1.916	2.058	1.0,0.6	2.267	2.442	2.182
0.4,0.8	1.502	2.066	2.024	1.0,0.8	2.561	2.633	2.179
0.4,1.0	1.856	2.213	2.003	1.0,1.0	2.88	2.719	2.16

tween the composition x and y as in Eq. (6).

For lattice matching to InP, the optical band-gap energy ranges from 0.72 to 1.42 eV due to the direct gap induced by the Γ-conduction minimum band $[E_{min}^c(\Gamma)]$ over the entire range of y. The experimental band gap has been reported from 0.74($\sim$0.75) eV to 1.35($\sim$1.41) eV at 300 K ($\sim$77 °K).[19–24] The $E_{min}^c(\Gamma)$ is much lower than $E_{min}^c(L)$ (ranging over 1.59–2.13 eV) and $E_{min}^c(X)$ (ranging over 2.19–2.36 eV). This indicates that $In_{1-x}Ga_xAs_{1-y}P_y$ lattice-matched to InP can be used for an ELED. As shown in Fig. 2, good agreement between the calculations and experiments[19–24] is obtained for the $E1$ band gap and Γ energy gap.

The optical gap for lattice-matching to GaAs varies in the range 1.51–1.97 eV and there is a direct-to-indirect transition at the large limit of y ($y>0.91$) due to $E_{min}^c(X)$. Another crossover between the L (ranging over 1.80–2.30 eV) and X (ranging over 1.97–2.13 eV) band is obtained around $y \approx 0.5$. Besides, the L (or X) band approaches the Γ band in the range of $y<0.5$ (or $y>0.5$) (see Fig. 3). Due to the access of the L (or X) band to the Γ band, especially the degeneracy between the Γ and X band at $y=0.91$, appreciable population transfer of electrons is to be expected from the Γ to L (or X) band and it will affect the electron mobility above room temperature. From this view of the band-gap structure of $In_{1-x}Ga_xAs_{1-y}P_y$ lattice-matched to GaAs, we suggest that this material is unsuitable as an ELED. To our knowledge, the experimental band gap for lattice-matching to GaAs has not been reported over the entire range of the y composition. Only theoretical data by CPA (Ref. 8) are available to compare with UTB values and there are some differences in the L (1.72–2.05 eV by CPA), X (1.92–2.28 eV by CPA), and Γ (1.41–1.88 eV by CPA) bands. In contrast to UTB data, the CPA calculation has predicted a direct optical band gap over the entire range of y for the lattice matched to GaAs.

The bowing behavior occurs differently for the Γ, L, and X energy gaps. The Γ energy gap shows consistently down-

ward bowing for both lattice-matching on InP and GaAs, but the bowing trends of the L and X energy gaps are not consistent. We found that the band bowing was dominantly led by the conduction-band minimum (CBM) rather than the valence-band maximum (VBM), which does not affect the bowing trends, even though the VBM fluctuated a little in the energy range of -0.045–0.006 eV for the lattice matched to InP and -0.067–0.060 eV for the lattice matched to GaAs over the entire range of y. The origin of band-bowing behavior in the alloy can be understood by examining the analytic expression of the TB scheme for the energy bands at the symmetrical points.[25,18] The diagonalization of the TB Hamiltonian matrix gives an exact analytic formula for the energy eigenvalues at the symmetric point (Γ, L, and X) and the conduction minimum values can be written by $E(\Gamma_{min}^c)=[Ess(000)0+ \ Ess(000)1]/2+ (\{[Ess(000)0-Ess(000)1]/2\}^2 \ +[4Ess(0.5,0.5,0.5)]^2)^{1/2}$ and $E(X_{min}^c)=[Ess(000)0+Exx(000)1]/2+(\{[Ess(000)0 -Exx(000)1]/2\}^2+[4Esx(0.5,0.5,0.5)01]^2)^{1/2}$ (see the notation in Table I). $E(L_{min}^c)$ does not have an exact formula, but it is expected to be a complicated form with the interaction integrals between p and p atomic orbitals compared with the other exact form of the L band. Taking these points into consideration, the Γ gap bowing in the $A_{1-x}B_xC_{1-y}D_y$ alloy is induced by the disordered Hamiltonian interaction between s and s atomic orbitals [in Eq. (4)] such as $\langle s|(1 -x)(1-y)yV_{ACD}+xy(1-y)V_{BCD}+\cdots|s\rangle$, etc. In the UTB interpretation, the interactions of s and s atomic orbitals due to bond alternations in the possible disordered units determine the Γ gap bowing and the X band gap is bowed by s-p interactions and the L band by p-p interactions with bond switching. As shown in Figs. 2 and 3, the total s-s interaction energy in the disordered units of the $In_{1-x}Ga_xAs_{1-y}P_y$ lattice matched to InP and GaAs consistently preserve the attractive-disorder energy over the entire y range, but X and L disordered energies by s-p and p-p interactions are not consistent (i.e., they could be attractive or repulsive disordered energy).
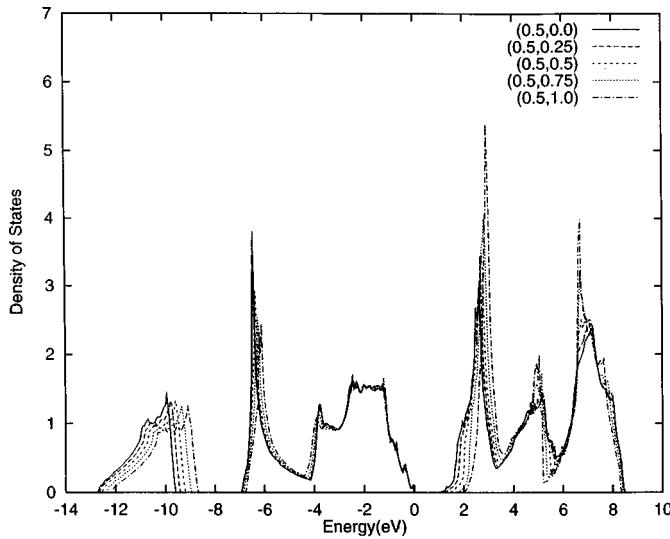
FIG. 4. Variation of the DOS for $In_{1-x}Ga_xAs_{1-y}P_y$ as a function of the change of the anion concentration y (0.0, 0.25, 0.5, 0.75, 1.0) for fixed cation concentration $x = 0.5$.

FIG. 5. Variation of the DOS for $In_{1-x}Ga_xAs_{1-y}P_y$ as a function of the change of the cation concentration x (0.0, 0.25, 0.5, 0.75, 1.0) for fixed anion concentration $y = 0.5$.

Figures 4 and 5 display the calculated DOS for fixed x and fixed y at 0.5 in the $In_{1-x}Ga_xAs_{1-y}P_y$ quaternary alloy. The band tail in the vicinity of the minimum of the conduction band diminishes by increasing the cation (or anion) mixing ratio. For fixed $y = 0.5$, we observe that the intensity of the first peak in the conduction band does increase significantly as x increases and there is no detectable change of the peak positions. But for fixed $x = 0.5$, the position of the first peak in the conduction bands changes appreciably to higher energy as y increases, while there is no detectable change of the intensity for the peaks of the DOS. We observe that the shift of the peak positions in the conduction band is mainly induced by alloy disorder from anion-site mixing rather than cation-site mixing in the $In_{1-x}Ga_xAs_{1-y}P_y$ quaternary alloy. In contrast, in the valence band, the cation-site mixing affects the peak position of the DOS and the anion-site mixing slightly changes the width and the intensity of the DOS. The peak position of the DOS in the valence band is shifted to higher energy as x increases for fixed y while the width and intensity of the DOS are influenced a little as y increases for fixed x. Also, the edge of the first valence band shifts from -6.78 to -7.25 eV with an increase in the cation mixing ratio, which induces the ionization energy of the alloy to increase by 0.47 eV for fixed $x = 0.5$ in the $In_{1-x}Ga_xAs_{1-y}P_y$. These qualitative observations of the DOS in the valence band agree with that of the CPA.[8]

IV. CONCLUSION

We demonstrated that the UTB methodology based on MPC can be readily applied to various quaternary alloy systems $A_{1-x}B_xC_{1-y}D_y$ by successfully presenting the energy band structure and DOS for $In_{1-x}Ga_xAs_{1-y}P_y$ alloys without any empirical input data. The UTB method based on MPC allows for a simplification of the complex problem, to reduce the computational efforts, and to investigate the utility of generic quaternary alloy systems. The freedom of exploration given by UTB should lead to the improvement and development of new devices. Following this logic, we have investigated how these techniques may be used for material design.[26]
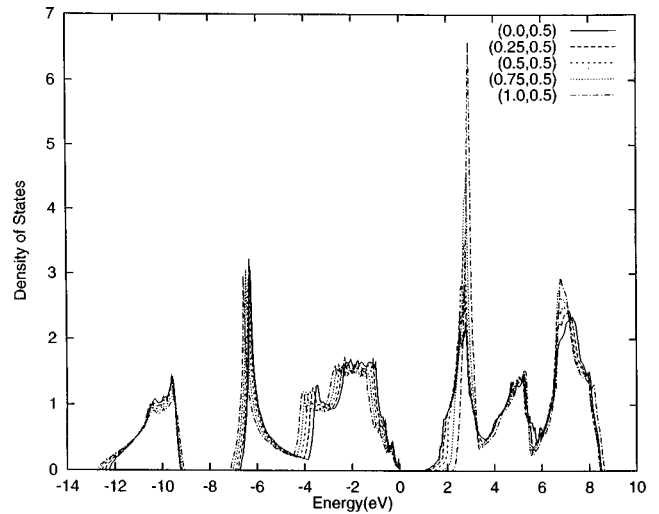
For the $In_{1-x}Ga_xAs_{1-y}P_y$ alloy system, we can summarize the findings as follows. (i) The band-gap range and extent of the bowing induced by disorder effects are governed by the differences of bond energies between the constituent binaries and the composition (x, y) for the alloy as in Eq. (6). A potential ELED material can be identified from the principal energy band-gap trends in a given range of compositions: an alloy that has the direct gap $[E(\Gamma)]$ being a considerable distance from the $E(L)$ and $E(X)$ band gaps can be used as a good ELED. (ii) The $In_{1-x}Ga_xAs_{1-y}P_y$ alloy lattice-matched to InP ($0 \leq x \leq 0.47$, $0 \leq y \leq 1.0$) has a direct optical gap induced by $E_{min}^c(\Gamma)$ at a considerable distance from $E_{min}^c(L)$ and $E_{min}^c(X)$, so that it is suggested to form a candidate ELED. In contrast, the direct-to-indirect transition induced by $E_{min}^c(X)$ occurs at $y = 0.91$, which is close to $E_{min}^c(\Gamma)$ for the lattice matched to GaAs ($0.55 \leq x \leq 1$, $0 \leq y \leq 1.0$), making it unsuitable for an ELED. (iii) The origin of the band-gap bowing can be understood as induced by the atomic orbital interaction due to the bond alternation; Γ-gap bowing is dominated by s-s, X-gap bowing by s-p, and L-gap bowing by p-p atomic orbital interactions through bond switching. (iv) For the cation and anion mixing effects on the DOS in the conduction band, the anion mixing plays an important role upon the shift of the peak positions and the cation mixing is more responsible for the change of the intensity and width of the peak. In contrast, cation and anion mixing play opposite roles in the valence band and there is good agreement with the results from the CPA.

[1] Maruice Quillec, *Materials for Optoelectronics* (Kluwer Academic, Boston, 1996).

[2] A. R. Adams, J. Allam, I. K. Czajkowski, A. Ghiti, E. P. O'Reilly, and W. S. Ring, *Strained-layers and Avalanche Photodetectors in Condensed Systems of Low Dimensionality*, edited by J. L. Beeby (Plenum, New York, 1991).

[3] R. N. Dupuis, J. C. Camphell, and J. R. Velebir, J. Cryst. Growth **77**, 598 (1986).

[4] M. A. Washington, R. E. Nahory, M. A. Pollack, and E. D. Beeka, Appl. Phys. Lett. **33**, 854 (1978).

[5] T. P. Pearsall, B. I. Millev, and R. J. Capik, Appl. Phys. Lett. **28**, 499 (1976).

[6] Kenichi Iga and Susumu Kinoshita, *Process Technology for Semiconductor Lasers* (Springer-Verlag, New York, 1996).

[7] P. S. Dutta and H. L. Bhat, J. Appl. Phys. **81**, 5821 (1997).

[8] A. B. Chen and A. Sher, Phys. Rev. B **19**, 3057 (1979).

[9] V. B. Gera, Rita Gupta, and K. T. Jain, Phys. Rev. B **36**, 9657 (1987).

[10] M. F. Ling and D. J. Miller, Phys. Rev. B **38**, 6113 (1988).

[11] S. Krishnamurthy, M. A. Berding, A. Sher, and A. B. Chen, Phys. Rev. B **37**, 4254 (1988).

[12] W. Porod, D. K. Ferry, and K. A. Jones, J. Vac. Sci. Technol. **21**, 965 (1982).

[13] K. Shim, D. N. Talwar, and H. J. Moh, Solid State Commun. **97**, 315 (1996).

[14] I. F. Chang and S. S. Mitra, Adv. Phys. **21**, 359 (1971).

[15] W. A. Harrison, *Electronic Structure and the Properties of Solids; Physics of the Chemical Bond* (Dover, New York, 1989); Svrre Foyen and W. A. Harrison, Phys. Rev. B **20**, 2420 (1979).

[16] J. C. Slater and G. F. Koster, Phys. Rev. **94**, 1498 (1954).

[17] K. Shim, J. W. Bae, S. W. Jeong, H. J. Moh, and D. N. Talwar, Solid State Commun. **98**, 825 (1996).

[18] D. N. Talwar and C. S. Ting, Phys. Rev. B **25**, 2660 (1982).

[19] E. O. Gobal, *GaInAsP Alloy Semiconductors*, edited by T. P. Pearsall (Wiley, Chichester, 1982), p. 295.

[20] P. M. Laufer, F. H. Pollack, R. E. Nahory, and M. A. Pollack, Solid State Commun. **36**, 419 (1980).

[21] K. Nakajima, A. Yamaguchi, K. Akita, and T. Kotani, J. Appl. Phys. **49**, 5944 (1978).

[22] H. Nagai and Y. Noguchi (unpublished).

[23] A. Lahtinen and T. Tuomi, Phys. Status Solidi B **130**, 637 (1985).

[24] O. Madelung, M. Schulz, and H. Weiss, *Numerical Data and Functional Relationships in Science and Technology; Semiconductors* (Springer, Berlin, 1982), Vol. 17.

[25] D. J. Chadi and M. L. Cohen, Phys. Status Solidi B **68**, 405 (1975).

[26] K. Shim and H. Rabitz (unpublished).